Published in: Microchemical Journal 141 (2018) 12–24

Detecting molecular changes in UV laser-ablated oil/diterpenoid resin coatings using micro-Raman spectroscopy and Laser Induced Fluorescence

Daniele Ciofini[a], Mohamed Oujja[b], Maria Vega Cañamares[c], Salvatore Siano[a], Marta Castillejo[b]

[a] Istituto di Fisica Applicata "N. Carrara", CNR, Via Madonna del Piano 10, 50019 Sesto Fiorentino, Italy
[b] Instituto de Química Física Rocasolano, CSIC, Serrano 119, 28006 Madrid, Spain
[c] Instituto de Estructura de la Materia, IEM-CSIC, Serrano 121, 28006 Madrid, Spain

Abstract

Naturally occurring diterpenoid resins were extensively applied, mainly as oily mixtures, through the ages as protective and decorative coatings on paintings, metals and wood artifacts. When these coatings age, tend to generate tougher films than triterpenoid resins, completely insoluble, increasingly subject to darkening, and then very hard to remove using conventional methods. In this regards, laser sub-micrometric ablative techniques are being increasingly used in the cultural heritage field also for the treatment of synthetic and natural polymer coatings. Here, in the wake of the positive outcomes achieved on triterpenoid resin films, the present approach has been applied and extended to diterpenoid resin coatings, which have never been thoroughly studied yet. In detail, colophony, sandarac and Manila copal resin films, prepared as solvent and linseed oil formulations, were subject to light-ageing and then systematically irradiated at various exposure conditions using the 4th (266 nm) and 5th (213 nm) harmonics of a Q-Switched Nd:YAG laser. UV-Vis absorption spectroscopy was used as preliminary characterization of the films optical properties. The assessment of physico-chemical modifications induced by artificial light-ageing and ns UV laser irradiation were assessed non-invasively by μ-Raman spectroscopy, Laser Induced Fluorescence (LIF) and microscopic examination.
The results underlined that, due to the presence of a polymer network, sandarac and copal resin coatings showed higher F_{th} than those composed of colophony. Morphologically, all the coatings were subject to bubbling upon 266 nm irradiation, while damage-free at 213 nm. At molecular level, irradiation at 266 nm produced minor changes to $\nu(CH_3)/\nu(CH_2)$, ν(C=O) and ν(C=C) modes, thus confirming an ablation mechanism mainly driven by photo-thermal bond-breaking through the ejection of gaseous by-products. Raman background fluctuations along with shifting and broadening of LIF maxima were supportive in the assessment of laser-induced surface modifications. Finally, the work performed indicates that the 213 nm wavelength is the most indicated for the treatment of aged solvent and oil diterpenoid-based coatings, as no side effects occurred. This outcome, corroborated by the previous results obtained in triterpenoid resin films, may have important implications in the field of cultural heritage conservation, as it extends the application range of solid-state Nd:YAG lasers to all types of protective and decorative terpenoid coatings.

Keywords: laser, ablation, diterpenoids, abietanes, pimaranes, labdanes,sandarac, copal, colophony, linseed oil

1. Introduction

Diterpenoid resins and derived products, such as, amber, sandarac, Venice turpentine, colophony and many varieties of copals and copaiba balsams, were extensively used through the ages for the formulation of protective and decorative coatings for paintings, metals (e.g bronze patination) and wood artifacts. Cennino Cennini, in his *Libro dell'Arte* around 1390, frequently mentions "vernice liquida" and "vernice comune" respectively as mixtures of sandarac/linseed oil and colophony/linseed oil, which were commonly used in Italy since the Middle Ages [1]. Eastlake, during its stay in Florence, concluded that "vernice liquida" was 'the ordinary term used by early writers, to designate the varnish for tempera pictures' and not simply an adjective describing the viscosity of the varnish [2]. Furthermore, copals were often used by Flemish painters to prepare varnishes and oil/resin paint media and, in the second half of the 19th century, in wood and musical instruments finishing, as they were tough and not susceptible to blooming [3][4]. Diterpenoids were extensively exploited also as additives to paint media (e.g. glazes, lacquers, Roberson's medium), for

preparing pigments (copper resinates), colored varnishes, mordant (e.g. adhesive for gold leaf), lining paste for repairing supports and for regeneration purposes [5][6][7][8][9].
Chemically, diterpenoids are composed of acids with a skeleton formed by bi- or tricyclic C20-hydrocarbon (four isoprene units). As depicted in **Error! Reference source not found.**, the main resin constituents include abietanes (ABA, NABA, PAA, LPIA) pimaranes (PIA, IPIA, SPIA) and various labdanes (agathic, torusol, larixol acids) [10][11]. Sandarac (*Tetraclinis articulata*) and Manila copal (*Agathis dammara*) resins are characterized also by a particularly reactive polymeric fraction consisting of COA (Fig.1) [10][12][13]. In contrast, diterpenoid resins containing pimarane- and abietane-type molecules do not polymerize spontaneously, as they have C=C bonds located in different positions.

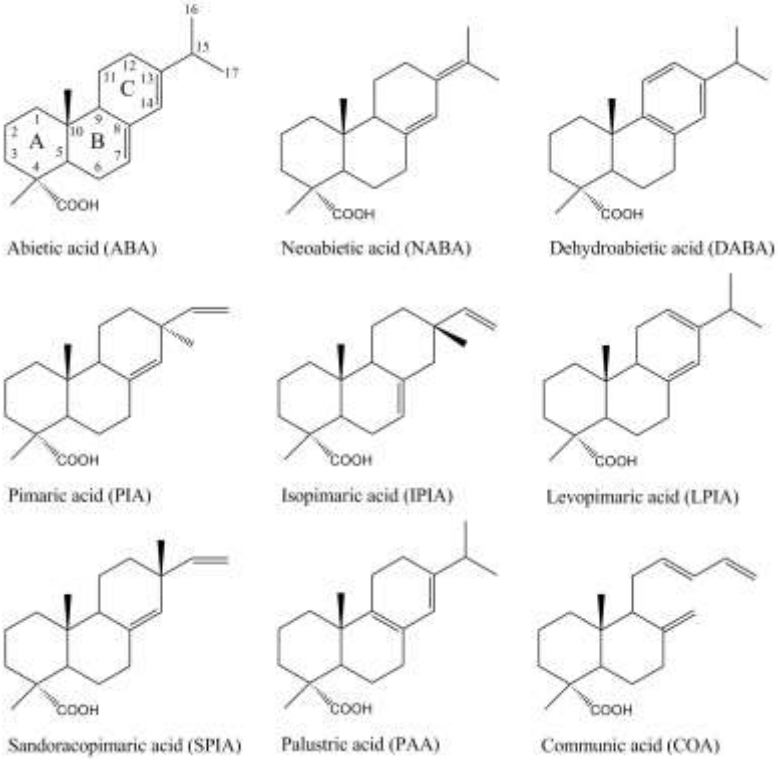

Figure 1 Skeleton types of the main diterpenoid acids found in conifer resins [9]. Ring numbering is depicted for abietic acid (ABA) according to common nomenclature.

Thanks to this composition, diterpenoid resin-based coatings possess higher propensity to generate tough films than triterpenoid resins (i.e. mastic and dammar). Besides, resin-cooking operations with drying oils, as routinely done in the past, and natural ageing mechanisms produce further compositional changes over time, thus making aged diterpenoid varnishes, especially oily mixtures, no longer soluble in most of common organic solvents, tough and optically darkened [14][15]. Long-standing methods of facing with this problem, still in use today, rely in combining mechanical means (e.g. scraping or lifting with a scalpel) with high polarity chemical stuff iteratively and carefully. Sometimes, this operation is even more complex due to the close similarity, in physical and chemical properties, with the binding medium of the underlying layers to be preserved. In this respect, gradual and selective removal of diterpenoid-based coatings from artworks is an issue deserving great attention on behalf of the conservation community. In this regards, safer and more controllable conservation strategies based on laser ablative treatments have been proposed from the mid-nineties and widely applied to date on metals, stones and painted artefacts [16][17]. With particular reference to the removal of synthetic and natural organic coatings, 1064 nm fundamental of Nd:YAG laser proved to be more effective in removing overpainted pigmented layers from paintings [18], whereas ultraviolet (UV) lasers in the ns, ps and fs domains have demonstrated to provide superior spatial resolution, control and safety in thinning down glazes and transparent varnish films [19][20]. An alternative approach, but completely different, is based on the photo-thermal disaggregation (i.e. explosive evaporation) of the treated surface using the combined action of free-running Er:YAG (2940 nm) lasers and wetting agents with OH-containing molecules [21]. However, results achieved on the removal of shellac varnish upon 213 nm laser

ablation have shown that this approach is the most indicated for the safe removal of the varnish layer, as no physicochemical modifications were induced either to varnish or underlying paint layers [22]. In the wake of these positive findings, a spectroscopic characterization of laser irradiation effects occurring at 213 and 266 nm in a set of naturally cured and artificially aged varnishes (i.e. mastic, dammar and shellac varnishes) was carried out using Micro-Raman spectroscopy, Laser Induced Fluorescence (LIF) and microscopic examinations [23]. From the results emerged that in contrast to 266 nm, surface morphology and varnish composition remained unaffected upon laser 213 nm treatments. To confirm these results and in view of possible application on actual artworks, the proposed approach has been extended for the first time for identifying the impact of UV laser radiation on a representative set of diterpenoid varnish coatings (colophony, sandarac and Manila copal), which were purposely-designed and characterized using the above-mentioned spectroscopic methodology. The novelty of the presented approach relies on extending the knowledge about laser-oil/diterpenoid coats interaction and finding a standalone laser technique for treating any type of light-sensitive coated surface, without the need of recurring to the use of wetting stuff, which otherwise might produce unwanted effects over time.

2. Material and methods

2.1 Laboratory samples

Varnish formulations were prepared according to the methodology accurately described in a previous study [15]. Colophony (Col-Eth) and sandarac standard (San-Eth) (marketed by Zecchi, Florence) pure resins were both dissolved in ethanol (30% w/v). Manila Copal being insoluble in most of organic solvent was prepared only as oily mixture. Oil-resin mixtures including colophony (Oil-Col), Sandarac (Oil-San) and Manila copal (Oil-Cop) were formulated by cooking method at high temperature. Linseed oil containing a cobalt drier was selected to reduce the induction time during the curing process. In detail, Oil-Col was softened, mixed with hot oil (120 °C), and then heated up to 220 °C for about 15 min while Oil-San and Oil-Cop were prepared in a similar way, early step by softening up to 150 °C and then heating up to 285 °C. Once the temperature dropped down to 60 °C, rectified turpentine oil was added in 1:1 ratio (wt:wt).
Afterwards, formulated varnishes were applied both on synthetic round quartz plates (2.5 cm diameter, 2.5 mm thick) by casting method and on primed canvas suitable for oil painting by brush. Since either solvent and oil varnishes take very long times to get completely dried, a set of reference samples were left to harden under controlled laboratory conditions (T= 20 ºC, R.H= 40-45%, cut-off of 380 nm) for about 24 months. Thus, the term reference in the text refers to samples naturally dried for 24-months, which cannot be properly considered extremely aged systems. A second set of samples, after one-month drying period from the preparation, was exposed to accelerated lighting conditions in a cw air-cooled Xenon test chamber (500 hours, B.S.T= 50 °C, cut-off of 290 nm, 50 mW/cm^2). Once artificial ageing was completed, the samples were exposed to free oxygen conditions for 6 months and then stored in the dark for about one year prior to be investigated.

2.2 UV-Vis absorption spectroscopy

UV-Vis absorption measurements, in terms of amount of material and thickness, were optimized to highlight the absorption features in the 200-400 nm range where the absorbance is three orders of magnitude greater than in the visible region. To this goal, few milligrams of resin were weighted (balance readability10^{-5} g), grinded and then dissolved in equal concentration of about 0.086 % (0.00259 g/3cc) (weight to volume) by selecting a suitable solvent or blend by Teas chart (see Table 1) [24][25].

Table 1 Varnish samples, after natural curing and artificial ageing, and solvents used for preparation along with the corresponding solubility properties

Sample	Solvent	Solubility[a]	Solvent	Solubility[a]

Reference			*Artificially aged*	
Col-Eth	trichloromethane	s.	trichloromethane	s.
San-Eth	isopropanol	s.	isopropanol/dcm (1:1)	p.s.
Oil-Col	trichloromethane	s.	trichloromethane	s.
Oil-San	isopropanol/dcm[b] (1:1)	s.	benzyl alcohol	i.
Oil-Cop	trichloromethane	p.s.	trichloromethane	p.s.
[a]s: soluble, p.s.: partially soluble, i: insoluble, [b]dcm: dicloromethane				

An ultrasonic bath was used to speed up the dissolution process. Afterward, a volume of about 3 ml was cast on round quartz plates (5 cm diameter, 2 mm thick). Once the films were dried and the solvent completely evaporated, the resulting thickness was measured using a Digital Comparator (Mahr Extramess) with a resolution of up to 0.2 µm. The measured values ranged between 1.5-2 µm. In this way, the spectra collected covered an absorbance range, which was well-below the spectrophotometer saturation threshold of 3 absorbance units. All the UV-Vis absorption spectra were collected using a Shimadzu UV3600 double-beam spectrophotometer. The spectral window was settled in a wavelength range of 200-800 nm with a sampling interval of 1 nm and a scan speed of 200 nm min^{-1}. The collected data were elaborated by plotting the mean absorption coefficient (α_{mean}) as a function of wavelength and no solvent subtraction was needed in order to correct the absorption profiles. First order derivatives were calculated over the whole spectral window in order to find the correct position of the inflection point, which provides useful information about the wavelength of maximum absorbance. Afterwards a slight (5 points) average-adjacent smoothing filtering was applied in order to improve the signal-to-noise ratio.

2.3 Laser testing methodology

Laser irradiation tests were carried out on quartz and grounded canvas substrates using the 4th (266 nm) and 5th (213 nm) harmonics of a Q-Switched (15 ns) Nd: YAG laser (Lotis II, LS-2147). The single-pulse ablation thresholds were determined by measuring the minimum incident laser pulse energy (E_{th}) at which gas desorption was observed from the sample surface. During these trials, the laser beam was focused on the surface of the varnish sample by means of a spherical plano-convex quartz lens (f=80 mm) and the laser pulse energy was adjusted by finely rotating a variable dielectric attenuator (Laser Optik). To avoid uncertainty of measurements deriving from the lateral extent of the laser-generated surface modifications on varnish film, the precise determination of the laser-spot size was performed on a photosensitive Polaroid film. Afterwards, by applying the spot regression method for Gaussian laser beam profiles, the beam radii ω_0 at both wavelengths were correctly calculated and then, the F_{th} for each varnish films derived [22][23][26] [27]. In this approach, the laser fluence, F, on the sample surface and the diameter, D, of the ablated area are related by $D^2 = 2\ \omega_0^2\ \ln(F/F_{th})$, where ω_0 is the $1/e^2$ radius of the Gaussian beam distribution and F_{th} is the ablation threshold. Once determined F_{th} as $E_{th}/\pi\ \omega_0^2$, for simulating cleaning tests, the samples were mounted on a motorized x-stage samples and then areas of about 10x6 mm^2 were automatically laser scanned using a cylindrical plano-convex quartz lens (f= 150 mm). The spot size was about 6.0x0.1 mm^2 at 213 nm and 5.5x0.1 mm^2 at 266 nm. The fluence was fixed at $F_{th} = 2F_{th}$, in order to maximize the ablation efficiency, in terms of ejected material per incident fluence unit, and at same time, to reduce the number of photons reaching the remaining varnish layer [28]. The repetition rate was settled at 10 Hz while scan-speeds at 0.1, 0.2 and 1 mm/s. In this way, the corresponding number of laser pulses/step applied for each laser spot were 10, 5 and 1, respectively. Using the $n = 1-l/2r$, where n is the pulse overlap, l is the length between the center of two successive laser spots and r the spot radius (half width of the rectangular laser spot, r= 0.05 mm), the pulse-overlap can be estimated. Considering the three scan speeds reported above the pulse overlaps were 90%, 80%, and 0 %, respectively. Chemical and physical modifications upon laser removal at 213 and 266 nm were evaluated on scanned areas at 0.1 mm/s (10 laser pulses, overlap 90 %) with a fluence of $2F_{th}$.

2.4 Micro-Raman spectroscopy

Micro-Raman analyses were performed on the varnish films applied on round quartz plates in order to study both the material photo-degradation processes and the laser-induced modifications. Micro-Raman spectra were recorded using a In Via Renishaw System (785 nm excitation wavelength) coupled to a confocal microscope. The Raman signal was calibrated using a standard Si target (520 nm emission line). The grating was 1200 lines/mm and the spectral resolution about 2 cm^{-1}. The excitation laser was focused onto the sample surface using a 50x (NA 0.55) objective lens allowing for a spatial (lateral) resolution down to 1 µm. 5 points of Savitzky Golay smoothing filters was applied to the recorded spectra, which are presented without any further processing, as ground subtraction and normalization.
As Raman signals and background may vary significantly depending on the varnish composition, preparation method and ageing, for all the prepared samples the measuring condition reported in Table 2 were used.

Table 2 Measuring conditions used for the µ-Raman analysis of prepared varnish samples. These conditions were exploited also for analyzing laser-ablated sample areas.

Sample	**Accumulations**	**Power (mW)**	**Acquisition time (s)**
Reference samples			
Col-Eth	3	10	15
Oil-Col	3	10	15
San-Eth	3	10	15
Oil-San	3	10	15
Light-aged samples			
Col-Eth	3	10	15
Oil-Col	1-3	50	15
San-Eth	3	10	15
Oil-San	1-3	50	15
Oil-Cop	1-3	50	15

For reference and light-aged solvent varnishes (Col-Eth and San-Eth) spectra of better quality were obtained using 10 mW. Due to the high Raman backgrounds, for light-aged oil varnishes it was necessary to increase the power up to 50 mW.

2.5 Laser Induced Fluorescence spectroscopy

Laser Induced Fluorescence (LIF) measurements were performed on reference and artificially aged varnish films applied on primed canvas, before and after laser irradiation, using an excitation wavelength of 266 nm, which is a sensitive probe for assessing the laser-induced modifications. LIF spectra were measured using a 0.30 m spectrograph with a 300 lines mm^{-1} grating (TMc300 Bentham) coupled to an intensified charged coupled detector (2151 Andor Technologies) providing a spectral coverage of 280 nm. The spectral range was centered around 450-500 nm and a 320 nm cut-off filter was used in order to reject the second order of emissions at lower wavelengths including the excitation one. The time gating was synchronized with the excitation laser pulse at 3 µs. The surface of the sample was illuminated at an incidence angle of 45° with a pulse energy less than 0.1 mJ and a spot of about 3 mm^2 (fluence of 3 mJ/cm^2). Each spectrum was the average of 20 measurements acquired in two different points of each irradiated area. The selected repetition rate was 1 Hz. All the recorded spectra were normalized to their maxima to be independent from the incident intensity and the quantity of analyzed material.

3. Results

3.1 UV-Vis absorption spectroscopy of non-irradiated varnish samples

In Figure 2 are displayed the UV-Vis absorption coefficients of the solvent-extractable material following natural curing and artificial ageing (see Table 1).

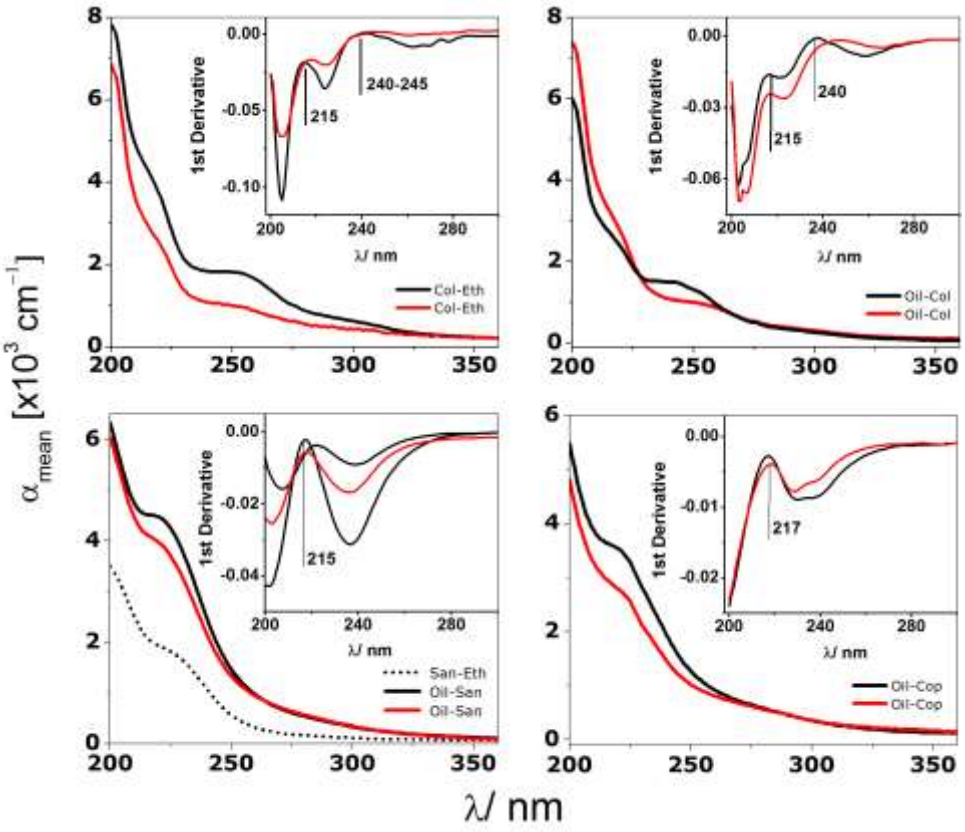

Figure 2 UV-Vis absorption coefficients and 1st derivative (inset graphs) of reference (black solid line) and light-aged (red solid line) diterpenoid varnish films.

Among the studied resins and oily mixtures, distinct absorption features deriving from the different number and position of C=C bonds may be observed. Col-Eth and Oil-Col varnish films, either reference or light-aged, showed a three-band structured absorption profile within which the position of each maximum is better appreciated in 1st derivative (Fig. 2, see inset). In detail, Col-Eth is characterized by a rather sharp negative peak at about 203 nm ($\alpha_{ref} \approx$ 6800 and α_{aged} = 6000 cm^{-1}) whose maxima are below 200 nm, a marked positive shoulder ($f' \neq 0$) at around 215 nm ($\alpha_{ref} \approx$ 4500 and α_{aged} = 2800 cm^{-1}), a low intensity absorption band ($f'=0$) at 240-245 nm ($\alpha_{ref} \approx$ 1800 and $\alpha_{aged} \approx$ 1100 cm^{-1}) and a very weak and wide band ($f' \neq 0$) at about 270-280 nm ($\alpha_{ref} \approx$ 700 cm^{-1}).

Similarly, the first intense negative peaks in Oil-Col are now wider and splitted, as a "tooth", in two unresolved bands at 203 ($\alpha_{ref} \approx$5340 and $\alpha_{aged} \approx$6750 cm^{-1}) and 206 nm ($\alpha_{ref} \approx$4065 and $\alpha_{aged} \approx$5235 cm^{-1}). The latter shoulder in both samples may be related to the presence of linseed oil. The positive shoulder ($f' \neq 0$) appears for both the samples at 215 nm. Different features were also noted in the 230-250 nm absorption region. In detail, the positive bands ($f'=0$) are located at 235 ($\alpha_{ref} \approx$1500 cm^{-1}) and 250 nm ($\alpha_{aged} \approx$1000 cm^{-1}) indicating a bathochromic shift from unaged to aged Oil-Col samples of 15 nm, respectively.

Sandarac and Manila copal varnish films have similar UV-Vis absorption features and can be well differentiated from colophony resin due to the apparently absence of abietane compounds, such as ABA and DABA, which is in agreement with their composition. 1st derivative spectra of San-Eth and Oil-San are characterized by a strong minimum at about 202-205 nm, whereas for Oil-Cop falls out the spectrophotometer limit. San-Eth showed the first positive peak at about 220 nm ($\alpha_{ref} \approx$1900 cm^{-1}), although the extracted fraction was very low. In fact, artificially aged San-Eth spectrum was not reported because the material is completely insoluble. On the opposite, Oil-San and Oil-Cop have the

peak mentioned above respectively at ~217 nm ($\alpha_{ref\text{-}aged}$≈4500-3820) and 218 nm ($\alpha_{ref\text{-}aged}$ ≈3650-3000). Both the latter are slightly shifted toward lower wavelengths in comparison to the unaged San-Eth sample.

3.2 Laser ablation thresholds and surface topography

To determine the laser ablation thresholds, we followed the procedure described in 2.3 section. Plotting D^2 versus lnE, E being the pulse energy, ω_0 was determined by linear fitting, taking the slope as equal to $2\omega_0^2$. The calculated value of ω_0 was 0.3 and 0.55 mm at 213 and 266 nm, respectively.
The single-shot values of F_{th} of varnish films, determined as $E_{th}/\pi\ \omega_0^2$, are reported in Figure 3a-b.

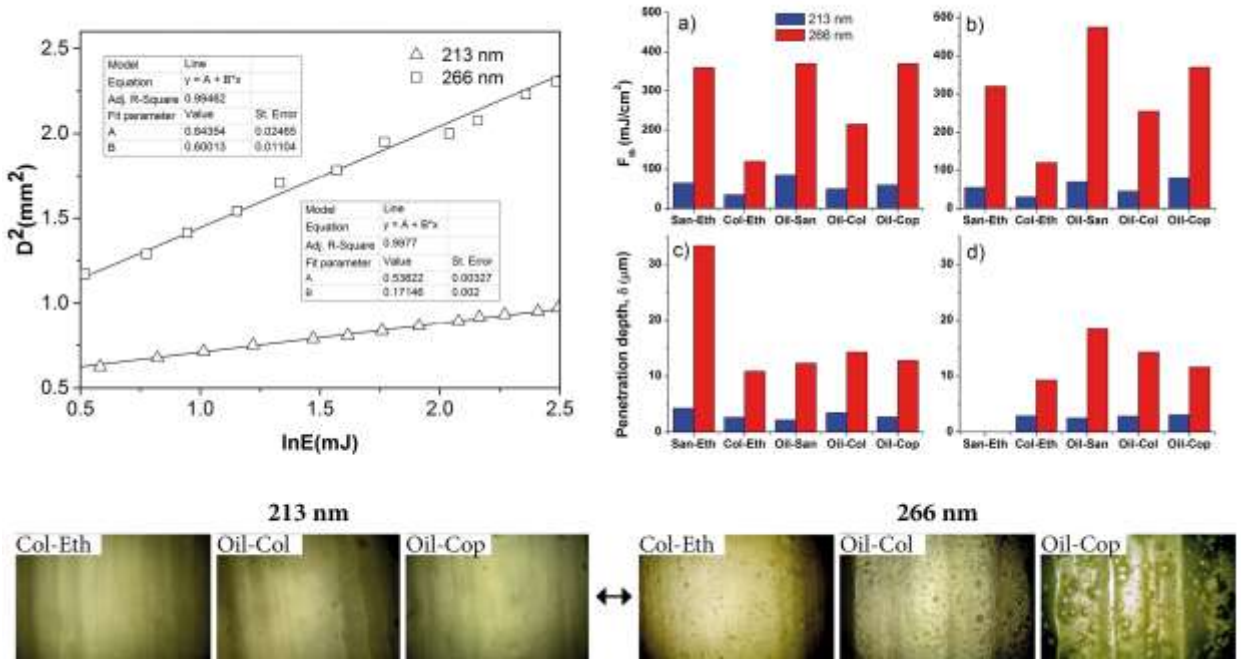

Figure 3 Semilog plot showing the linear dependence of D^2 versus lnE at 213 and 266 nm (pulses of 15 ns) on Polaroid film. Single-pulse Fth (mJ/cm²) and optical penetration depth, δ (μm) measured on reference (a-c) and artificially aged (b-d) varnish films. The estimated error on F_{th} is less than 5 %. Micrographs (magnification 50x) showing surface topography of ablated aged varnish films. The size of each picture is 120x180 μm².

As already stated for triterpenoid varnish films [23], both F_{th} and penetration depths (δ)Oi, are markedly different at the two wavelengths, in general from 3 to 6 times higher at 266 nm. Most importantly, for 266 and 213 nm, F_{th} values are dependent on the type of resin present in the varnish. Surface topography upon irradiation was analyzed by using confocal microscopy and some representative micrographs are shown in Fig. 3. As for triterpenoid varnishes, irradiation of varnish films at 213 nm did not produce surface modifications to the remaining varnish layer, which preserved its natural gloss. Contrarily, formation of microsized bubbles and whitish appearance were observed at 266 nm, even though number and size distribution of bubbles varied depending on the type of varnish formulation and degree of polymerization. Bubbles of about 5-15 μm were observed mostly in varnish films containing "hard resins", such as sandarac and copal. Oil-based varnishes showed even more pronounced bubbles than those prepared without oil. Moreover, especially in colophony samples, bubbles were smaller with respect to pimarane and labdane-rich films due to the lower penetration depth. Irradiation at 266 nm was also accompanied with darkening, which was well appreciable to the naked eye.

3.3 Characterization of varnish samples by micro-Raman spectroscopy

3.3.1 Non–irradiated samples

μ-Raman spectra measured on reference and light-aged samples are displayed in Fig. 4 and main Raman peaks listed in Table 3. First, reference and light-aged varnish samples showed spectra typical of a complex multicyclic oxidized composition that is formed upon drying and ageing [29][30]. Remarkable changes were observed in the background, which, especially in light-aged samples, overlapped the Raman signals up to making them unidentifiable. A detailed description of Raman spectra, based on the type of resin, is provided in the following sections.

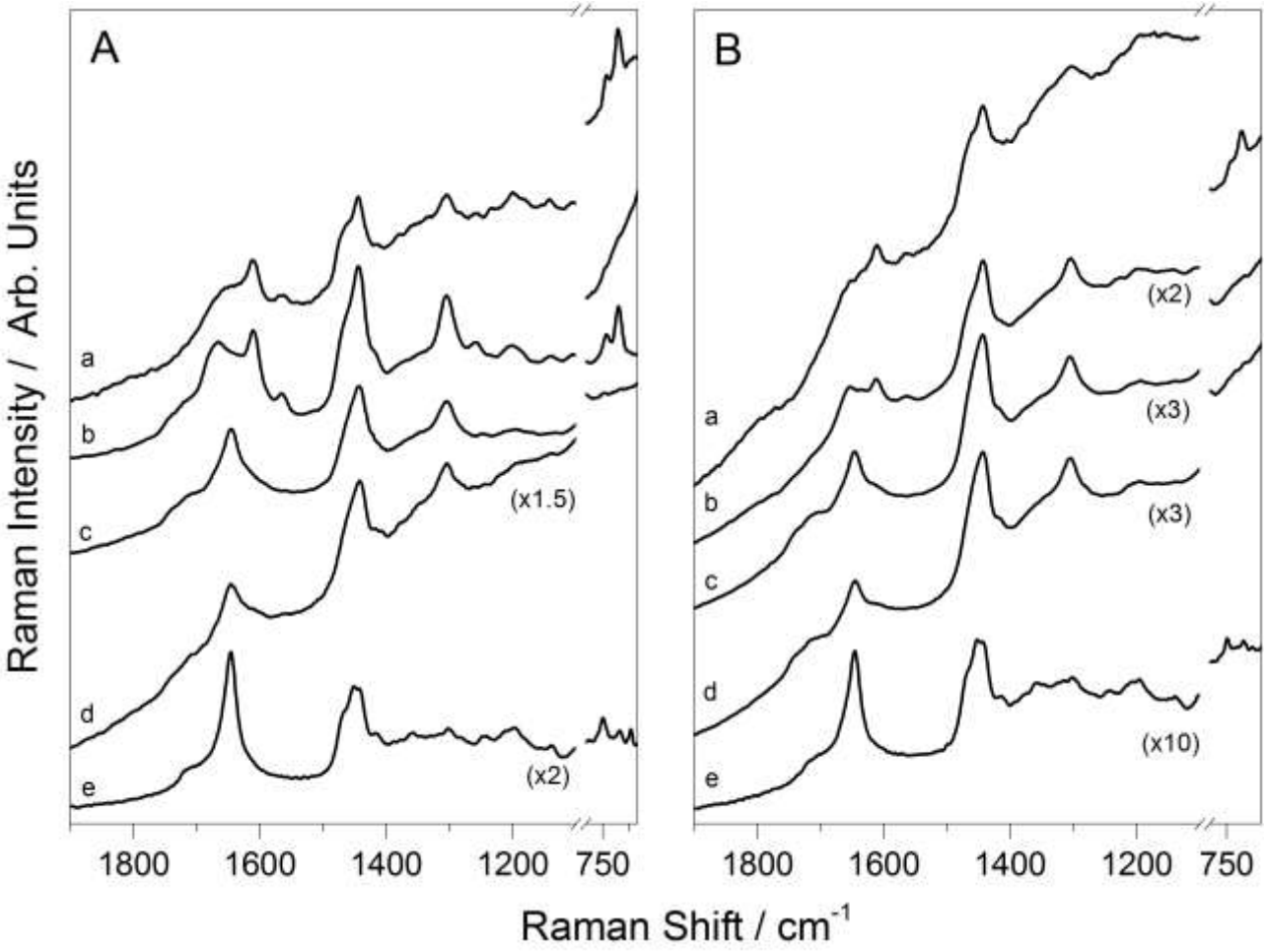

Figure 4 μ-Raman spectra of reference (A) and light-aged (B) varnish films. Lower case letters in the graphs refer to Col-Eth (a), Oil-Col (b), Oil-Cop (c), Oil-San (d) and San-Eth (e).

Table 3 Raman band positions of the prepared varnish coatings. The assignments correspond to the spectral region showed in Fig.4

Sample	**Raman shift (cm^{-1})**	**Spectrum**
Reference samples		
Col-Eth	1652, 1612, 1565, 1468, 1444, 1304, 1282, 1259, 1200, 1181, 1142, 740, 705	Fig.4A, a
Oil-Col	1740, 1715, 1665, 1610, 1565, 1468, 1442, 1304, 1258, 1204, 1142, 740, 705	Fig.4A, b
Oil-Cop	1737, 1710, 1644, 1360, 1301, 1249, 1190, 1140	Fig.4A, c
Oil-San	1740, 1710, 1646, 1442, 1415, 1302	Fig.4A, d
San-Eth	1716, 1646, 1464, 1450, 1442, 1415, 1360, 1301, 1246, 1211, 1195, 1138, 750, 701, 670	Fig.4A, e
Light-aged samples		
Col-Eth	2927, 2872, 1652, 1611, 1565, 1444, 1305, 705	Fig.4B, a
Oil-Col	2930, 2872, 1715, 1654, 1636, 1612, 1565, 1469, 1442, 1304, 1258, 1201, 1072, 1051, 1000, 929, 883, 740, 705	Fig.4B, b
Oil-Cop	1742, 1709, 1644, 1442, 1301, 1190, 1063	Fig.4B, c

Oil-San	1740, 1710, 1646, 1444, 1415, 1302, 1200, 1062	Fig.4B, d
San-Eth	1716, 1700, 1646, 1450, 1442, 1415, 1355, 1302, 1244, 1195, 1138, 748, 701	Fig.4B, e

Colophony

In reference Col-Eth, the band assigned to trans-conjugated ν(C=C) in ABA (Fig.1) at 1652 cm^{-1} was observed, but slightly overlapped by hidden bands of isolated C=C at 1670 and 1636 cm^{-1} ascribed to pimaranes (IPIA, PIA, SPIA), which are typically detected both in fresh and in aged *Pinus* resins. As shown in Figure 1, pimaranes are slightly different in basic structure and stereochemistry if compared to abietanes and most importantly, lacking of conjugated C=C bonds, they do not contribute significantly to oxidation reactions. Conversely, degradation of colophony and Venice turpentine is predominantly the result of the oxidation and dehydrogenation of conjugated dienes of the abietane moiety [31]. Highly oxidized DABA compounds resulting from dehydrogenation of ABA were found in old painting varnishes [32][33][34] and Stradivari's instruments [4]. Thus, the higher peak intensity of DABA at 1611 cm^{-1} highlighted that reference Col-Eth samples (24 months-old) were moderately aged [35][36][37][38][39]. This feature may be appreciated also in light-aged Col-Eth, even though the higher spectral background and the most advanced skeletal deterioration did not allow a reliable comparison with reference Col-Eth films. Nonetheless, changes and intensity decreases of the bands at 2927 and 2869 cm^{-1} assigned to stretching vibrations of CH_2/CH_3 groups in Col-Eth samples (see Fig. 5a and b) indicated molecular changes in agreement with their photo-oxidation pathway [15].

Concerning to reference Oil-Col films, due to the presence of oil and the heat processing, several variations in the Raman spectrum were observed. Markedly modified resulted the C=C stretching bands at 1665 cm^{-1} in Oil-Col samples, probably due to the contribution of isolated C=C bonds present in polyunsaturated fatty acids chains. Moreover, a shoulder at ca. 1710-1725 cm^{-1} was evident and ascribable to C=O stretching of the oil component or of a ketocarbonyl group in position 7 (7-oxodehydroabietic and 15-hydroxy-7-oxodehydroabietic). Further minor changes were ascribed to $\delta(CH_{2\text{-}3})$ at 1304 cm^{-1} and to δ(CCH) and =C-H in plane at 1200 cm^{-1}. Unexpectedly, spectral features of light-aged Oil-Col samples revealed appreciably different. The peak at 1665 cm^{-1} disappeared as much as to detect the peak at 1654 $cm^{-1}$of ABA [34][37]. However, the band shift observed, from 1665 to 1654 cm^{-1}, could be most likely related to a change in the configuration of isolated C=C in fatty acids chains upon light ageing [40].

Sandarac and copal

The main spectral variations between reference and aged samples (Figure 4A and B) were ascribed to C=C and C=O stretching vibrations along with other minor features. In particular, in light-aged San-Eth sample, the intensity of the peak at 1646 cm^{-1} assigned to conjugated ν(C=C) in the vinyl group of COA decreased and that of δ(CH) at 1452 cm^{-1} slightly increased with respect to reference San-Eth. Basically, the opening of the C=C bonds and the increase of the peaks related to bending deformation of CH_2/CH_3 groups are the result of cross-linking and cleavage (β-scission or oxidative scission) reactions upon ageing [13]. These modifications led also to an increase of the Raman background, which can be mostly related to the higher fluorescence of newly formed compounds [41]. Further minor modifications in San-Eth samples can be observed in the fingerprint. In light-aged San-Eth, the peaks at 750, 701 and 670 cm^{-1} ascribed to skeletal vibrations resulted slightly modified. As regards oily mixtures (Oil-San and Oil-Cop samples), spectra resulted drastically changed in shape and band positions with respect to San-Eth samples (Fig. 4), more smooth and peaks partly hindered by the background, which tends to increase strongly upon varnish heating and light-ageing [41]. Furthermore, the C=C/CH ratio related to the peaks at 1646 and 1452 cm^{-1}, in light-aged Oil-San and Oil-Cop, appeared considerably decreased due to the significant conversion of C=C bonds into single bonds. As mentioned above, C=C bonds are active site both for cross-linking and scission reactions. Together with these reactions, light ageing produced also an increase of oxidized compounds (i.e. carboxylic groups, ester linkages, ketones) which can be appreciably observed from the more pronounced and broadened shoulders in the C=O region (1740-1710 cm^{-1}) of light-aged Oil-San and Oil-Cop.

3.3.2 Laser irradiated samples

Colophony

Although apparently Col-Eth and Oil-Col samples do not show significant spectral changes in terms of band position, laser irradiation induced structural modifications in some extent.

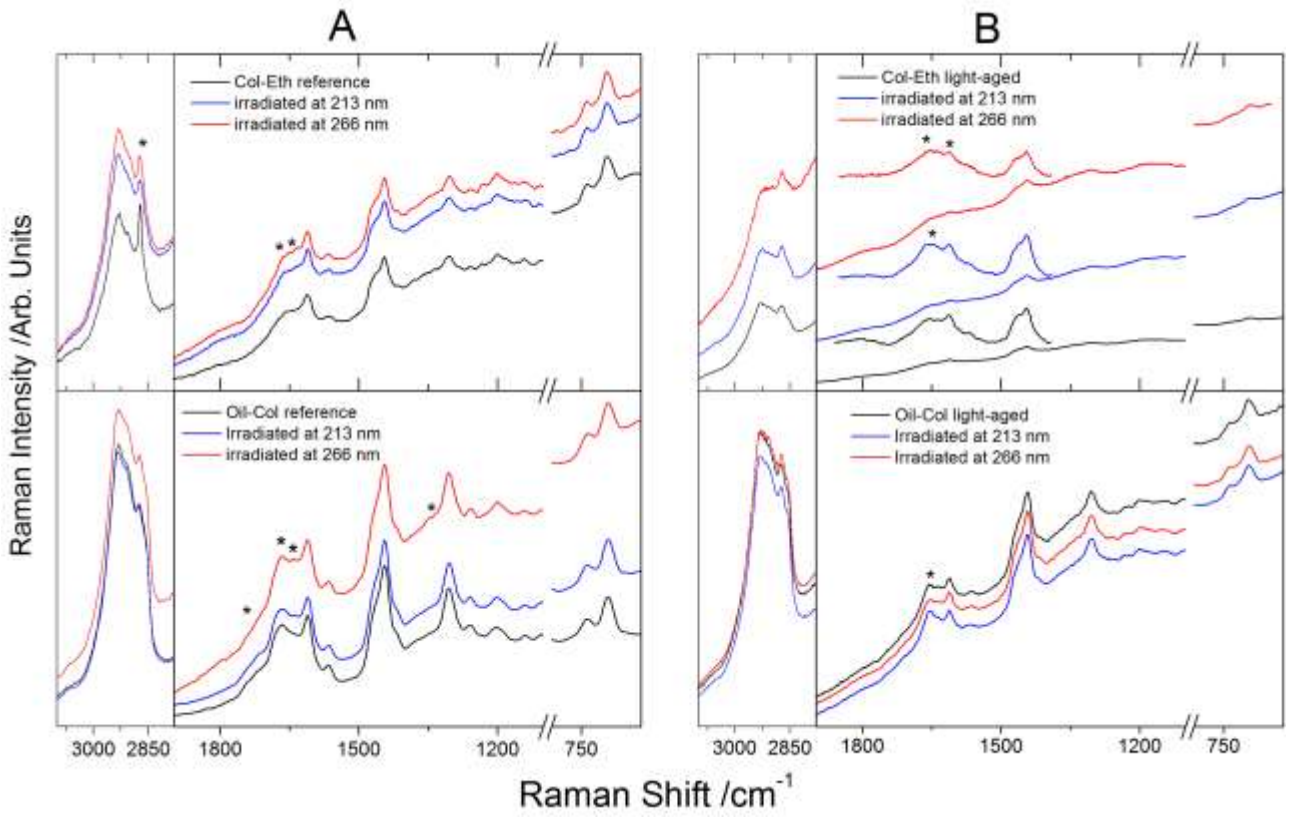

Figure 5 μ-Raman spectra of reference (A) and light-aged (B) colophony films before and after laser irradiation. Asterisks refer to laser-induced modifications.

In the 3000-2800 cm^{-1} region, the peak at 2869 cm^{-1} related to *ν*(CH) in Col-Eth decreased at both wavelengths, in accordance to the variation observed among reference and light-aged non-irradiated samples. Moreover, subtle modifications of the shoulder at 1650 cm^{-1} assigned to abietane and pimarane moieties may be appreciated. In aged Col-Eth the peak at 2927 cm^{-1} of *ν*(CH) was prominently reduced at 266 nm. Background subtracted inset graphs covering the 1400-1850 cm^{-1} were added to show the most representative changes (Fig. 5), otherwise not detectable in aged Col-Eth. With respect to reference Col-Eth, the region of *ν*(C=C) of ABA at 1652 cm^{-1} and the peak at 1611 cm^{-1} assigned to DABA appeared slightly changed, in particular at 266 nm. For instance, during heating, abietanes are known to isomerize readily, predominantly to ABA and dehydroabietic (DABA), while LPIA may disappear [42][32]. Concerning Oil-Col samples, a distinct alteration pathway with respect to Col-Eth was observed. Reference Oil-Col experienced background increases upon laser irradiation, especially at 266 nm, whereas for light-aged Oil-Col the trend was different and appreciably opposite. However, such a behavior could be ascribed to the advanced state of deterioration of light-aged Oil-Col samples, as much as to show insensitivity to laser radiation. Besides this, peaks at 1710 and 1665 cm^{-1} in reference Oil-Col irradiated at 266 nm appeared in same extent slightly modified. These modifications can be related to minute changes in the C=O and C=C stretching modes, respectively, which are related to the oil and pimarane moieties. Moreover, the Raman bands related to the C-C skeletal vibrations of the abietane and pimarane structures, at 740 and 705 cm^{-1}, did not undergo any change upon laser irradiation using both laser wavelengths [38].

Sandarac and copal

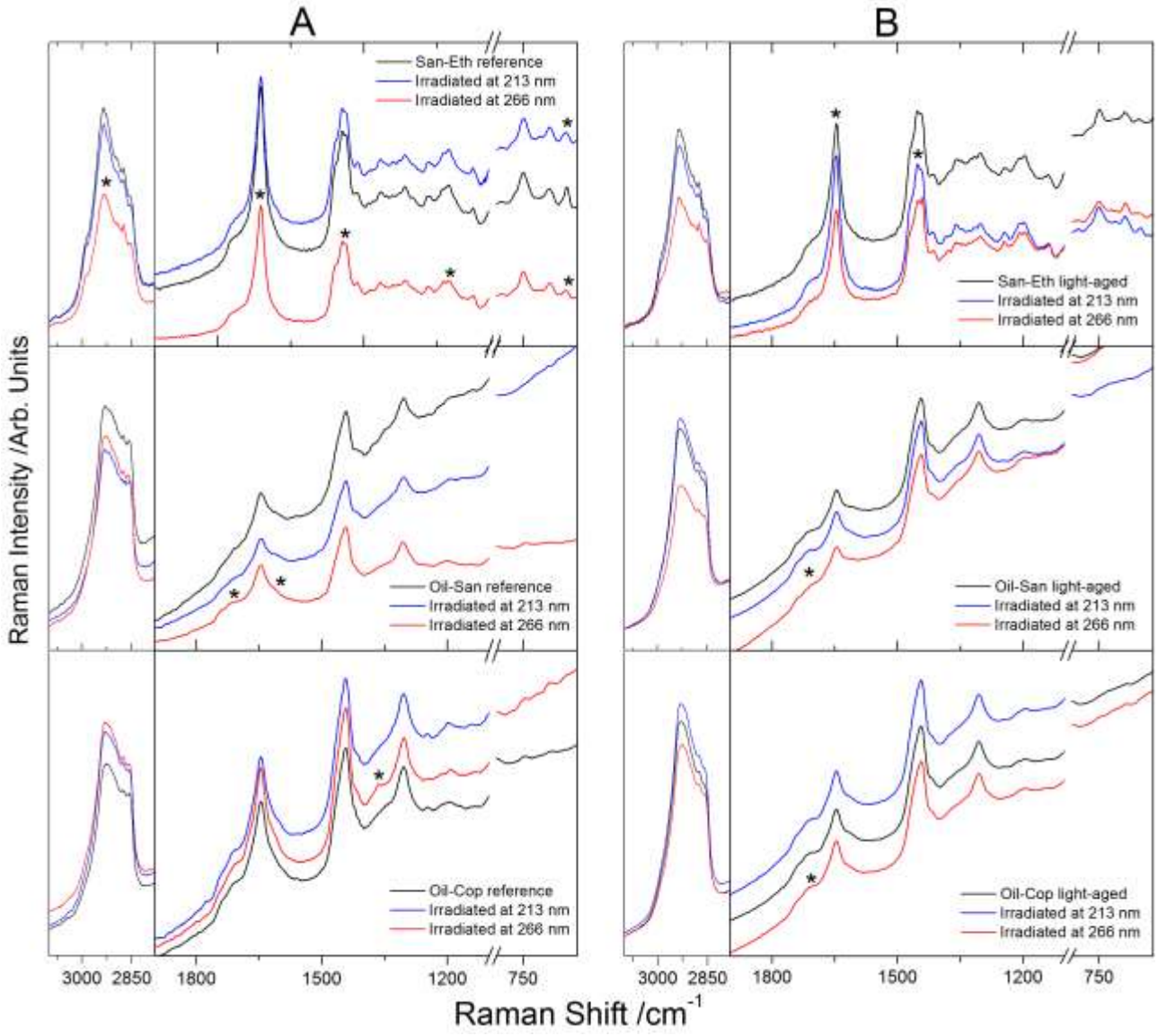

Figure 6 μ-Raman spectra of reference (A) and artificially (B) aged varnish films before (dark line) and after laser irradiation at 213 (blue line) and 266 (red line) nm.

In detail, laser irradiation at 266 nm of reference San-Eth produced a marked intensity decrease of the whole spectrum without inducing significant changes in the spectral distribution. As displayed in fig.7 the main Raman peaks related to C-H, C=O, C=C stretching modes remained almost unaffected. Moreover, the ν(C=C)/δ(CH) ratio (1646/1450 cm^{-1}) increased slightly from 1.8 to 1.9. Regarding light-aged San-Eth, a similar intensity decrease of the spectrum was observed upon irradiation at 266 nm. A decrease of the ν(C=O) at 1710 cm^{-1} may be better appreciated in the normalized spectrum of Figure 7. Additional changes concerned the decrease of ν(C=C) at 1646 cm^{-1} and $\nu(CH_{2\text{-}3})$ at 2933 cm^{-1} bands. Instead, ν(C=C)/δ(CH) ratio (1646/1450 cm^{-1}) in light-aged San-Eth changed from 1.4 to 1.35 upon 266 nm irradiation and from 1.4 to 1.45 upon 213 nm irradiation.

Reference Oil-San experienced an evident decrease of the Raman background with respect to the other oily mixtures, most likely due to a less oxidized composition in depth. Nonetheless, unlike the other samples, the shoulders of ν(C=O) at 1710 and 1740 cm^{-1} increased in intensity and broadened upon 266 nm laser

treatment and became more similar to those of non-irradiated light-aged Oil-San. This modification can be better appreciated in the normalized spectra of Figure 7. On the contrary, the same shoulders in light-aged Oil-San were subject to a remarkable decrease upon 266 nm laser irradiation.

In reference Oil-Cop, laser-induced modifications were almost negligible except for a minor change ascribed to the formation of a band at 1364 cm^{-1} assigned to the $\delta(CH_2)$ and $\delta(CH_3)$, which appeared after irradiation at 266 nm. Instead, it was noticed that in light-aged Oil-San and Oil-Cop samples, ablation at 266 nm generated a reduction of the shoulder bands at 1710 and 1740 cm^{-1} belonging to carbonyl functionalities of resin and oil, respectively.

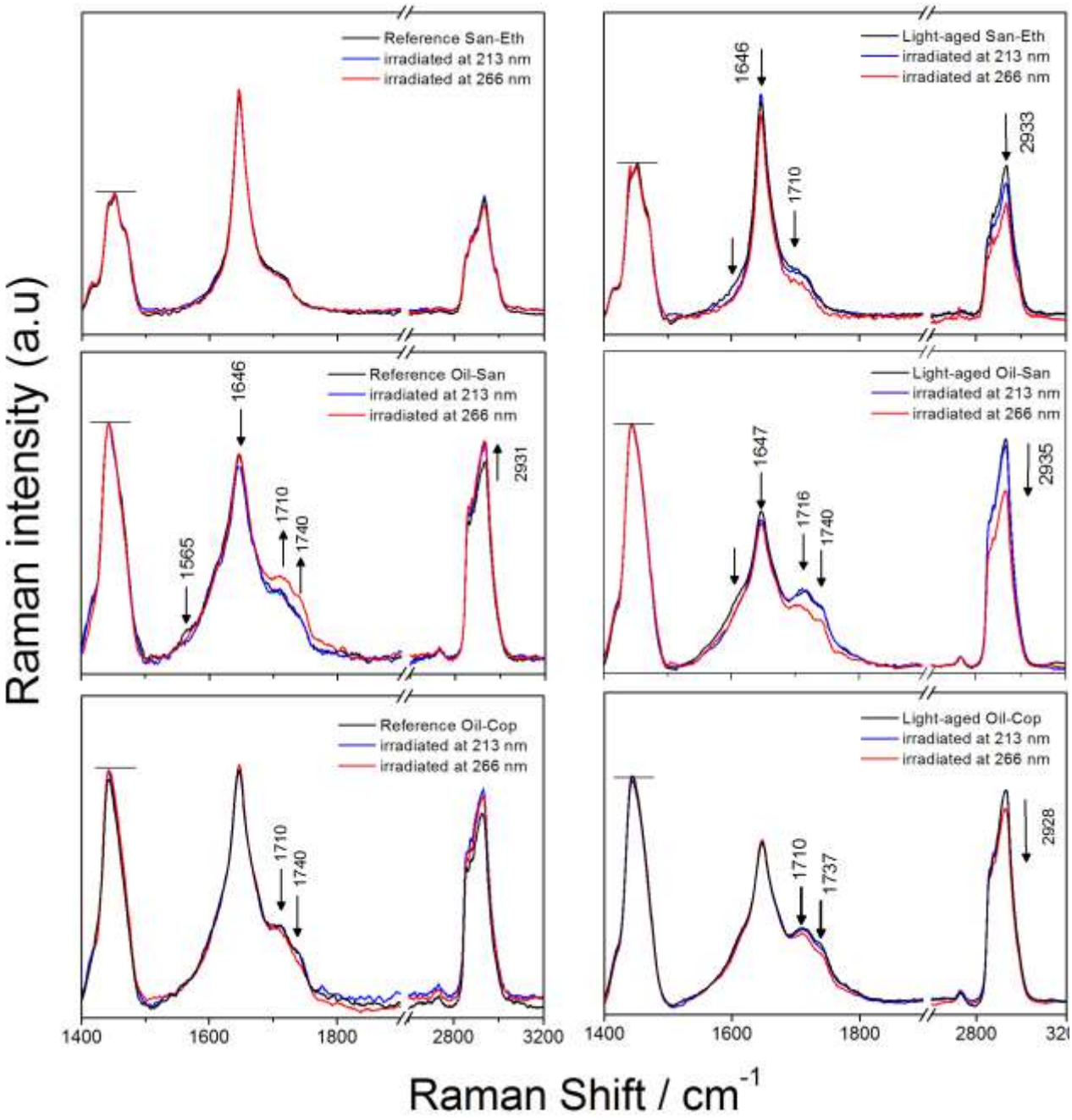

Figure 7 Background subtracted and normalized (at 1445 cm^{-1}) Raman spectra of non-irradiated and laser-irradiated (2 F_{th}, 10 pulses) varnish films. Arrows indicate the bands affected by laser irradiation treatments.

Particularly affected in this region was light-aged Oil-San and to a lesser extent light-aged Oil-Cop, which experienced an unperceivable reduction of C=O and C-H. Variations ascribed to samples irradiated at 213 nm were almost negligible in most cases.

3.4 Fluorescence Induced Fluorescence measurements

3.4.1 Non-irradiated areas

Normalized LIF emission spectra of reference and light-aged varnish samples at laser excitation wavelength of 266 nm are shown in Fig. 8. Fluorescence maximum (λ_{max}) of the underlying ground was at 435 nm and LIF intensity was strongly lower than that relative to the varnish layers.

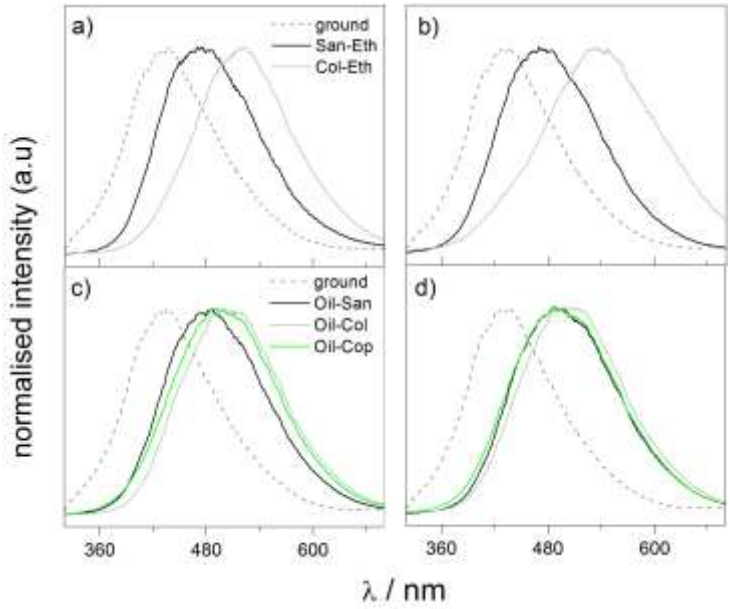

Figure 8 Normalised LIF spectra (excitation at 266 nm) of reference (a,c) and light-aged (b,d) varnish samples. Dotted lines show the fluorescence emission of the underlying layer (ground).

Reference and aged San-Eth samples showed λ_{max} at 478 and 485 nm, whereas their FWHM values were 139 and 145 nm, respectively. The slight broadening of LIF band in San-Eth samples suggests accumulation of some oxidation products upon light-ageing, therefore indicating a relatively large stability. Instead, Col-Eth revealed higher susceptibility to light-aging, as due to the formation of new fluorophores, spectral features resulted drastically broadened and red-shifted. FWHM varied from 140 to 172 nm and λ_{max} from 520 to 532 nm. Very surprisingly, λ_{max} of reference and aged oil varnishes (pre-heated in linseed oil) resulted almost unchanged, especially once light-aged. Conversely, FWHM varied for reference and aged samples between 142 and 152 nm for Oil-San and for Oil-Col and between 147 and 156 nm for Oil-Cop.

3.4.2 Irradiated areas

Chemical modification upon UV laser removal of varnish films were also assessed by LIF measurements on scanned areas irradiated with $2F_{th}$ and 10 laser pulses. For comparison, LIF spectra after normalization to respective λ_{max} are dispayed in Fig. 9.

It is first observed that, in most cases, samples etched at 213 nm showed negligible LIF variations, in terms of λ_{max} shifting and band broadening. Appreciable variations were those measured on light-aged Col-Eth and San-Eth varnish films, which experienced blue-shifts of about 15 and 10 nm, respectively. With respect to solvent-based varnishes, no changes were assessed in reference and light-aged oil samples, thus suggesting that oil varnishes are compositionally more uniform across the thickness. Irradiation at 266 nm produced remarkable modifications to all the processed varnishes. Likewise to 213 nm, the most sensitive was Col-Eth. For the latter, LIF spectra resulted strongly blue-shifted and broadened. In detail, λ_{max} between reference and light-aged Col-Eth samples shifted from 520 to 480 nm and from 532 to 485 nm, whereas FWHM became greater with values of 50 and 35 nm. San-Eth, either reference and light-aged, revealed higher stability and the changes observed were similar to those of San-Eth samples treated at 213 nm. Contrarily, it is noteworthy that oil samples showed both blue and red-shifts of λ_{max} upon 266 nm irradiation. Reference and light-aged Oil-Col and Oil-Cop red-shifted around 15-20 nm, whereas Oil-San blue-shifted around 10 nm. Actually, red-shifting may be considered effectively a chemical modification due to laser irradiation, as it means formation of new conjugated C=C bonds.

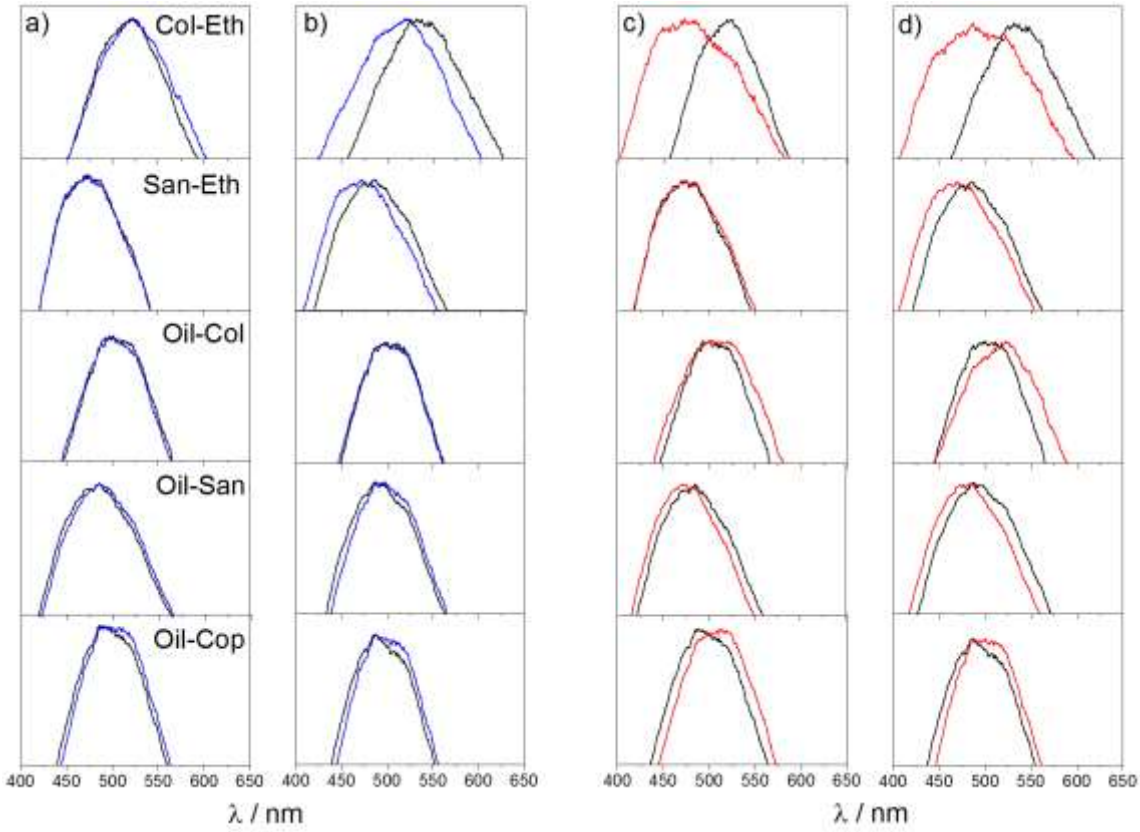

Figure 9 LIF spectra of reference (a,c) and light-aged (b,d) varnish films before (black line) and after laser irradiation at 213 (blue line) and 266 (red line) nm using $2F_{th}$ and 10 pulses

4. Discussion

In this work, Raman and LIF measurements have provided reliable information about the assessment of physico-chemical modifications induced by artificial light-ageing and by ns UV laser irradiation. Moreover, preliminary analysis of extractable components by means of UV-Vis absorption spectroscopy proved to be essential for material characterization and supportive to study absorption features at the laser wavelengths used. The results achieved are herewith discussed on the basis of the resin type forming the varnish film.

4.1 Colophony

UV-Vis absorption profiles of Col-Eth films were characterized by a three-structured absorption profile due to the high content of abietane compounds. The marked shoulder band at 210-215 nm could be ascribed to pimaranes (PIA, IPIA and SPIA), which are present in colophony in minimal amount and absorb in that region due to presence of a vinyl group side-chain [11]. Likewise, DABA has a strong absorption at 200 nm, and a less intense shoulder at 218-220 nm. Concerning with the broad shoulder band at 240-245 nm, which is missing in sandarac and copal-based films, previous studies have shown by capillary electrophoresis that the different position of two conjugated C=C double bonds in ABA and NABA is responsible for a clear UV absorption maximum at 240 nm and 250 nm, respectively [11,43]. Moreover, due to the high reactivity of C-H groups next to conjugated C=C bonds in ABA, a further contribution to absorption in this region may come from the formation of α,β-unsaturated ketones. The weakest absorption band at about 270-280 nm ($n \rightarrow \pi^*$ transition) may be assigned to LPIA acid [35][44]. According to the UV-Vis absorption profiles, the comparison of derived δ between 213 and 266 nm revealed to be appreciably different among the varnishes studied. These differences influenced oppositely both the surface modifications and single-pulse value of ablation threshold F_{th}, which were significantly and expectedly higher at 266 nm with respect to 213 nm. Thanks to the high absorptivity at 213 nm and to the low propensity of abietanes (ABA, NABA, PAA and LPIA) to polymerize, colophony films showed very low ablation thresholds (F_{th}=30-40 mJ/cm^2) in

comparison to sandarac and copal films (F=80-100 mJ/cm^2). Topographically, in all the sample tested, irradiation at 266 nm produced micro-sized features (bubbling). This phenomenon, ascribed to the production of gaseous molecules (CH_3OH, CH_4, $HCOOCH_3$, CO, and CO_2), has never been observed in terpenoid varnishes upon irradiation at 213 nm. As a matter of fact, it is well-known that, as a photo-thermal bond-breaking mechanism takes place on synthetic polymers at wavelengths longer than 240 nm with ns, ps and fs pulse duration [45–47]. Chemically, blackening of Col-Eth films upon irradiation at 266 nm can be explained as the result of the thermal decomposition of the abietane skeleton. It was reported that dehydrogenation of ABA to DABA is only the early stage, as it is followed by decarboxylation to give dehydroabietin and by a full aromatization to retene [48][49]. The latter compound can be rarely found in naturally aged varnishes but it can be considered as a stable and dark by-product formed upon strong heating. However, μ-Raman spectroscopy was unable to detect the presence of such compounds in the remaining darkened colophony films, mainly due to the strong background emission of light-aged samples.
Basically, slight changes of $\nu(CH_3)/\nu(CH_2)$, C=O and C=C bonds were observed upon UV laser-treatments and were larger at 266 than at 213 nm. These alterations can be associated, either in terpenoid coatings [23] and on polymers [45], with similar initiating unzipping reaction (hydrogen abstraction, depolymerization) and/or direct photolysis of methyl/methylene groups, esters and carbonyl structures. Instead, fluctuations of Raman background upon laser treatments at 213 and 266 nm rose, in most cases, positively. As demonstrated by the variations occurring between reference and light-aged films, it is likely possible to ascertain that rising in the slope and counts of the fluorescence background are attributable to structural alterations and formation of newly oxidized species . Results from LIF measurements underlined that blue-shifts and broadening upon laser irradiation in Col-Eth samples were mostly related to the uncovering of less oxidized layers. Contrarily, films ablated at 266 nm showed also red-shifts and band broadening ascribed to the formation of new conjugated C=C bonds and accumulation of oxidation products. In colophony, due to its tendency to dehydrogenation and aromatization, a similar behavior was put in evidence upon light-ageing.

4.2 Sandarac and Copal

Sandarac and copal, being constituted mainly of pimarane and free labdane molecules, showed distinct UV-Vis absorption profiles with respect to colophony, according to the different number and position of C=C bonds in their carbon skeletons. Main forming acids, such as COA, agathic acid (R=COOH) and its monomethyl ester have a weak absorption at 240 nm ascribable to the conjugated diene side-chain [12,50]. However, as the results have shown, the absorption contribution of C=C side chain in COA can be reasonably neglected, as during all the steps leading to film formation (i.e. heat processing, polymerization and light-ageing), the conversion of C=C bonds into simple C-C bonds takes place. Therefore, the shoulders at 216-220 nm may be attributed to pimarane moieties (PIA, IPIA and SPIA). This conversion occurs also in polyunsaturated fatty acids chain [10], even though the remaining monounsaturated (oleic) and saturated acids (stearic, palmitic) do not contribute significantly to the general absorption in the near-ultraviolet.
As consequence of these compositional differences, reference and light-aged San-Eth, Oil-San and Oil-Cop films have shown at both laser irradiation wavelengths of 213 and 266 nm higher F_{th} values than colophony-based films. Thereby, the presence of a polymer network would explain the fluctuations observed in F_{th}, by outlining the boundary between “soft” and “hard” resins. Sandarac and copal resins were definitely more resistant to laser radiation at both wavelengths (i.e higher F_{th}), but bubbling is produced upon 266 nm irradiation. In relation to these surface modifications, Raman analyses have shown reduction to ν(CH), δ(CH), ν(C=O) and ν(C=C) modes of resin and oil, and other minor components. In contrast, no or subtle spectral variations were assessed in films ablated at 213 nm. Background variations behaved oppositely with respect to abietanes, with effects of major entity at 266 nm. Background decreasing could be mostly related to the reduction/ablation of the varnish thickness and to the presence of a stepped drying/ageing gradient. LIF measurements underlined red-shifting and band broadening at 266 nm and negligible variations at 213 nm, especially for non-aged samples. In this regards, non-linear optical microscopy imaging techniques has been recently used to address and evaluate the induced structural and photochemical modifications that take place in terpenoid varnish films upon UV laser irradiation [19]. In detail, dammar varnish coatings applied

on a sensitive substrate were irradiated using different wavelengths (266, 248 and 213 nm) and pulse durations (ns, ps and fs). By supporting what observed here on diterpenoid coatings, it was demonstrated that highly absorbed UV photons, namely those at 213 nm, are effective in thinning down the dammar layer without modifying the fluorescence properties neither of the varnish nor of the layer underneath.

Conclusions

In the present work physico-chemical modifications induced by artificial light-ageing and by nanosecond UV laser irradiation (213 and 266 nm) on diterpenoid resin-based coatings were assessed non-invasively by μ-Raman spectroscopy, Laser-Induced-Fluorescence and microscopic examination. The results underline that the prepared resin films were more susceptible and subject to molecular and surface modifications (darkening and bubbling) upon irradiation at 266 nm than at 213 nm. Chemically, irradiation at 266 nm produced minor changes to $\nu(CH_3)/\nu(CH_2)$, $\nu(C=O)$ and $\nu(C=C)$ modes, thus indicating an ablation mechanism mainly driven by photo-thermal bond-breaking accompanied with the ejection of gaseous by-products. Furthermore, Raman background fluctuations and shifting and broadening of LIF maxima were supportive in the assessment of changes induced both by artificial light-ageing and laser irradiation. Additionally, changes occurring during artificial light-ageing were in turn useful for the interpretation of those caused by laser ablation. Finally, the work indicates that the 213 nm-wavelength, thanks to a non-thermal ablative channel (i.e. photochemical), is the most appropriate for the treatment of aged solvent- and oil-diterpenoid coatings. Surface properties of samples treated at 213 nm resulted topographically superior with respect to those observed using the wavelength of 266 nm. Besides these important advantages, the use of 213 nm is also promising for safety issues, as the hazards associated with skin and eye exposure are negligible with respect to 266 nm. In conclusion, the positive results achieved at 213 nm on diterpenoid resin-based coatings allow stating that such a laser-assisted sub-micrometric ablative approach may be definitely applied for the treatment of all types of terpenoid coatings, by extending the application range of the 213 nm quintupled Q-Switched Nd:YAG laser output in the cultural heritage field. Lastly, the laser-assisted approach proposed may be considered as an alternative to the use of free-running Er:YAG laser, especially whenever surface pre-wetting should be preferably avoided.

Acknowledgements

The present work was supported by Program Geomateriales 2 (S2013/MIT-2914) financed by Comunidad de Madrid and Structural Funds (FSE and FEDER), by the Integrated Platform for the European Research Infrastructure on Cultural Heritage (IPERION-CH) Ref. H2020-INFRAIA-2014-2015 nº 654028, by the Ministerio de Economía, Industria y Competitividad (MINECO) of Spain under Projects CTQ2016-75880-P and FIS2014- 52212-R, and by PEGASO project (POR FSE 2007-2013) funded by the Tuscany Region. M. O. thanks CSIC for a contract.

References

[1] E.R. De La Rie, Old master paintings: a study of the varnish problem, Anal. Chem. 61 (1989) 1228A–1237A. doi:10.1021/ac00196a003.

[2] J.M. Reifsnyder, A note on a traditional technique of varnish application for paintings on panel, Stud. Conserv. 41 (1996) 120–122.

[3] A.E. Rheineck, Drying oils in varnishes, J. Am. Oil Chem. Soc. 36 (1959) 574–582. doi:10.1007/BF02641152.

[4] J.P. Echard, L. Bertrand, A. Von Bohlen, A.S. Le Hô, C. Paris, L. Bellot-Gurlet, B. Soulier, A. Lattuati-Derieux, S. Thao, L. Robinet, B. Lavédrine, S. Vaiedelich, The Nature of the extraordinary finish of Stradivari's instruments, Angew. Chemie - Int. Ed. 49 (2010) 197–201. doi:10.1002/anie.200905131.

[5] G.L. Stout, R.J. Gettens, Painting Materials: A Short Encyclopaedia, Dover Publications; New edition (November 2, 2011), 1946.

[6] M.P. Merrifeld, Original Treatises on the Arts of Painting, Dover Publications, 1967.

[7] V. Dorge, F.C. Howlett, Painted Wood: History and Conservation, Getty Conservation Institute, 1998.

[8] J.S. Mills, R. White, The Organic Chemistry of Museum Objects, Butterworth-Heinemann, 1999.

[9] L. de Viguerie, P.A. Payard, E. Portero, P. Walter, M. Cotte, The drying of linseed oil investigated by Fourier transform infrared spectroscopy: Historical recipes and influence of lead compounds, Prog. Org. Coatings. 93 (2016) 46–60. doi:10.1016/j.porgcoat.2015.12.010.

[10] K.J. Van Den Berg, J.J. Boon, I. Pastorova, L.F.M. Spetter, Mass spectrometric methodology for the analysis of highly oxidized diterpenoid acids in Old Master paintings, J. Mass Spectrom. 35 (2000) 512–533. doi:10.1002/(SICI)1096-9888(200004)35:4<512::AID-JMS963>3.0.CO;2-3.

[11] A. Findeisen, V. Kolivoska, I. Kaml, W. Baatz, E. Kenndler, Analysis of diterpenoic compounds in natural resins applied as binders in museum objects by capillary electrophoresis., J. Chromatogr. A. 1157 (2007) 454–61. doi:10.1016/j.chroma.2007.05.010.

[12] R.M. Carman, D.E. Cowley, R.A. Marty, Diterpenoids. XXV. Dundathic acid and polycommunic acid, Aust. J. Chem. 23 (1970) 1655–1665.

[13] D. Scalarone, M. Lazzari, O. Chiantore, Ageing behaviour and analytical pyrolysis characterisation of diterpenic resins used as art materials: Manila copal and sandarac, J. Anal. Appl. Pyrolysis. 68-69 (2003) 115–136. doi:10.1016/S0165-2370(03)00005-6.

[14] S. Tirat, J.-P. Echard, A. Lattuati-Derieux, J.-Y. Le Huerou, S. Serfaty, Reconstructing historical recipes of linseed oil/colophony varnishes: Influence of preparation processes on application properties, J. Cult. Herit. 27 (2017) S34 – S43. doi:https://doi.org/10.1016/j.culher.2017.08.001.

[15] D. Ciofini, J. Striova, M. Camaiti, S. Siano, Photo-oxidative kinetics of solvent and oil-based terpenoid varnishes, Polym. Degrad. Stab. 123 (2016) 47–61. doi:10.1016/j.polymdegradstab.2015.11.002.

[16] S. Siano, J. Agresti, I. Cacciari, D. Ciofini, M. Mascalchi, I. Osticioli, A.A. Mencaglia, Laser cleaning in conservation of stone, metal, and painted artifacts: State of the art and new insights on the use of the Nd:YAG lasers, Appl. Phys. A Mater. Sci. Process. 106 (2012) 419–446. doi:10.1007/s00339-011-6690-8.

[17] P. Pouli, M. Oujja, M. Castillejo, Practical issues in laser cleaning of stone and painted artefacts: Optimisation procedures and side effects, Appl. Phys. A Mater. Sci. Process. 106 (2012) 447–464. doi:10.1007/s00339-011-6696-2.

[18] S. Siano, I. Osticioli, A. Pavia, D. Ciofini, Overpaint removal from easel paintings using an LQS Nd:YAG laser: The first validation study, in: Stud. Conserv., 2015: pp. S49–S57. doi:10.1179/00393630152.000000000207.

[19] M. Oujja, S. Psilodimitrakopoulos, E. Carrasco, M. Sanz, A. Philippidis, A. Selimis, P. Pouli, G. Filippidis, M. Castillejo, Nonlinear imaging microscopy for assessing structural and photochemical modifications upon laser removal of dammar varnish on photosensitive substrates, Phys. Chem. Chem. Phys. 19 (2017) 22836–22843. doi:10.1039/C7CP02509B.

[20] M. Oujja, M. Sanz, E. Rebollar, J.F. Marco, C. Domingo, P. Pouli, S. Kogou, C. Fotakis, M. Castillejo, Wavelength and pulse duration effects on laser induced changes on raw pigments used in paintings, Spectrochim. Acta - Part A Mol. Biomol. Spectrosc. 102 (2013) 7–14. doi:10.1016/j.saa.2012.10.001.

[21] L. Pereira-Pardo, C. Korenberg, The use of erbium lasers for the conservation of cultural heritage. A review, J. Cult. Herit. 31 (2017) 236–247. doi:10.1016/j.culher.2017.10.007.

[22] M. Oujja, A. García, C. Romero, J.R. Vázquez de Aldana, P. Moreno, M. Castillejo, UV laser removal of varnish on tempera paints with nanosecond and femtosecond pulses., Phys. Chem. Chem. Phys. 13 (2011) 4625–4631. doi:10.1039/c0cp02147d.

[23] D. Ciofini, M. Oujja, M.V. Cañamares, S. Siano, M. Castillejo, Spectroscopic assessment of the UV laser removal of varnishes from painted surfaces, Microchem. J. 124 (2016) 792–803. doi:10.1016/j.microc.2015.10.031.

[24] G. Hedley, Solubility parameters and varnish removal a survey, Conserv. 4 (1980) 12–18. doi:10.1080/01410096.1980.9994931.

[25] C. V Horie, Materials for Conservation: Organic Consolidants, Adhesives and Coatings, Butterworth-Heinemann, 2010.

[26] M.J. Liu, Simple technique for measurements of pulsed Gaussian-beam spot sizes, Opt. Lett. 7 (1982) 196–198. doi:10.1364/OL.7.000196.

[27] S. Baudach, J. Bonse, W. Kautek, Ablation experiments on polyimide with femtosecond laser pulses, Appl. Phys. A Mater. Sci. Process. 69 (1999) 395–398. doi:10.1007/s003399900276.

[28] C. Theodorakopoulos, V. Zafiropulos, Depth-profile investigations of triterpenoid varnishes by KrF excimer laser ablation and laser-induced breakdown spectroscopy, Appl. Surf. Sci. 255 (2009) 8520–8526. doi:10.1016/j.apsusc.2009.06.012.

[29] P. I., Isomerization of resin Acids During Distillation of Pina Oleoresin, Chem. Eng. Sci. 51 (1996) 2577–2582. http://ac.els-cdn.com/0009250996001170/1-s2.0-0009250996001170-main.pdf?_tid=e89caf78-b61f-11e4-a2ad-00000aab0f6c&acdnat=1424121069_b33b1a6eacce1f7a272d98e1bd5e8970.

[30] K.B. Anderson, New Evidence Concerning the Structure , Composition , and Maturation of Class I (Polylabdanoid) Resinites, in: Amber, Resinite, Foss. Resins, ACS Symposium Series, 1996: pp. 105–129.

[31] J.R. Hanson, The aromatisation of terpenes and steroids by dehydrogenation, J. Chem. Res. 39 (2015) 127–133.

[32] I. Pastorova, K.. van der Berg, J.. Boon, J.. Verhoeven, Analysis of oxidised diterpenoid acids using thermally assisted methylation with TMAH, J. Anal. Appl. Pyrolysis. 43 (1997) 41–57. doi:10.1016/S0165-2370(97)00058-2.

[33] M.V. Russo, P. Avino, Natural products such as adhesives in oil paintings, Nat Prod Res. 6419 (2016) 1–14. doi:10.1080/14786419.2015.1126263.

[34] V. Beltran, N. Salvadó, S. Butí, T. Pradell, Ageing of resin from Pinus species assessed by infrared spectroscopy, Anal. Bioanal. Chem. 408 (2016) 4073–4082. doi:10.1007/s00216-016-9496-x.

[35] M. Nuopponen, S. Willför, A.S. Jääskeläinen, A. Sundberg, T. Vuorinen, A UV resonance Raman (UVRR) spectroscopic study on the extractable compounds of Scots pine (Pinus sylvestris) wood: Part I: Lipophilic compounds, Spectrochim. Acta - Part A Mol. Biomol. Spectrosc. 60 (2004) 2953–2961. doi:10.1016/j.saa.2004.02.008.

[36] R.H. Brody, H.G.M. Edwards, A.M. Pollard, Fourier transform-Raman spectroscopic study of natural resins of archaeological interest, Biopolym. - Biospectroscopy Sect. 67 (2002) 129–141. doi:10.1002/bip.10059.

[37] I. Osticioli, D. Ciofini, A.A. Mencaglia, S. Siano, Automated characterization of varnishes photo-degradation using portable T-controlled Raman spectroscopy, Spectrochim. Acta - Part A Mol. Biomol. Spectrosc. 172 (2017) 182–188. doi:10.1016/j.saa.2016.03.016.

[38] V. Beltran, N. Salvadó, S. Butí, G. Cinque, T. Pradell, Markers, Reactions, and Interactions during the Aging of Pinus Resin Assessed by Raman Spectroscopy, J. Nat. Prod. 80 (2017) 854–863. doi:10.1021/acs.jnatprod.6b00692.

[39] I. Osticioli, D. Ciofini, A.A. Mencaglia, S. Siano, Warm white LED lighting in museums: Ageing effects on terpenoid resins assessed through Raman spectroscopy and chemometrics, Strain. (2017) e12255. doi:. https://doi.org/10.1111/str.12255.

[40] A. Schönemann, H.G.M. Edwards, Raman and FTIR microspectroscopic study of the alteration of Chinese tung oil and related drying oils during ageing, Anal. Bioanal. Chem. 400 (2011) 1173–1180. doi:10.1007/s00216-011-4855-0.

[41] O.R. Montoro, M. Taravillo, M. San Andrés, J.M. De La Roja, a. F. Barrero, P. Arteaga, V.G. Baonza, Raman spectroscopic study of the formation of fossil resin analogues, J. Raman Spectrosc. 45 (2014) 1230–1235. doi:10.1002/jrs.4588.

[42] J. Mills, R. White, Natural resins of art and archaeology their sources, chemistry, and identification, Stud. Conserv. 22 (1977) 12–31. doi:10.2307/1505670.

[43] J.H.T. Luong, T. Rigby, K.B. Male, P. Bouvrette, Derivatization of resin acids with a fluorescent label for cyclodextrin-modified electrophoretic separation, J. Chromatogr. A. 849 (1999) 255–266. doi:10.1016/S0021-9673(99)00503-8.

[44] W.H. Schuller, R.N. Moore, R. V. Lawrence, Air Oxidation of Resin Acids. II. The Structure of Palustric Acid and its Photosensitized Oxidation, J. Am. Chem. Soc. 82 (1960) 1734–1738. doi:10.1021/ja01492a049.

[45] E. Rebollar, G. Bounos, M. Oujja, C. Domingo, S. Georgiou, M. Castillejo, Influence of polymer molecular weight on the chemical modifications induced by UV laser ablation., J. Phys. Chem. B. 110 (2006) 14215–14220. doi:10.1021/jp061451u.

[46] E. Rebollar, S. Pérez, M. Hernández, C. Domingo, M. Martín, T. a Ezquerra, J.P. García-Ruiz, M. Castillejo, Physicochemical modifications accompanying UV laser induced surface structures on poly(ethylene terephthalate) and their effect on adhesion of mesenchymal cells., Phys. Chem. Chem. Phys. 16 (2014) 17551–17559. doi:10.1039/c4cp02434f.

[47] P. Pouli, a. Nevin, a. Andreotti, P. Colombini, S. Georgiou, C. Fotakis, Laser assisted removal of synthetic painting-conservation materials using UV radiation of ns and fs pulse duration: Morphological studies on model samples, Appl. Surf. Sci. 255 (2009) 4955–4960. doi:10.1016/j.apsusc.2008.12.049.

[48] D.E. Baldwin, V.M. Loeblich, R.A.Y. V Lawrence, Acidic Composition of Oleoresins and Rosins, 3 (1955) 342–346.

[49] N. Marchand-Geneste, a. Carpy, Theoretical study of the thermal degradation pathways of abietane skeleton diterpenoids: Aromatization to retene, J. Mol. Struct. THEOCHEM. 635 (2003) 55–82. doi:10.1016/S0166-1280(03)00401-9.

[50] G. Büchi, J.J. Pappas, Terpenes. I. Structure and Synthesis of the $C_{17}H_{20}$ Hydrocarbon Obtained by Dehydrogenation of Agathic Acid, J. Am. Chem. Soc. 76 (1954) 2963–2966. doi:10.1021/ja01640a031.